ACS APPLIED POLYMER MATERIALS

Editors' Choice
Open Access
This article is licensed under CC-BY 4.0
pubs.acs.org/acsapm

Article

# Biodegradable 3D Electronics from Growth-Induced Shape Change in Engineered Living Materials

Jared A. Gibson, Sasha M. George, Cedric P. Ambulo, Manivannan Sivaperuman Kalairaj, Yoo Jin Lee, Melbs LeMieux, Christopher E. Tabor, and Taylor H. Ware*

Cite This: https://doi.org/10.1021/acsapm.5c02855

Read Online

ACCESS | Metrics & More | Article Recommendations | Supporting Information

**ABSTRACT:** Engineered living materials (ELMs) are materials that derive their functionality from living and nonliving components. This study investigates the use of ELMs, specifically living yeast encapsulated in hydrogel substrates, as an approach to grow and transfigure 3D electronics. We developed three-dimensional (3D), transient electronic devices by integrating conductive metal inks, made of printable silver and liquid metal, onto ELMs. The ELMs undergo programmable growth based on induced environmental stimuli and transform from flat substrates into various programmed 3D shapes of various curvature, such as stretchable helices with a tunable pitch from 14.7 ± 3.05 to 65 ± 6 °/mm. These ELM substrates were found to be fully degradable over the course of 48 h in accelerated hydrolytic conditions, leaving behind only the conductive traces. Our findings indicate that yeast-based ELMs can effectively support electronic functionalities while being fully degradable, offering a promising alternative for growing 3D electronics and advancing sustainable electronics.

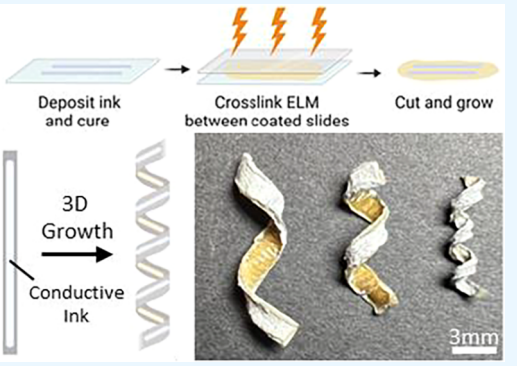


**KEYWORDS:** *engineered living materials, 3D electronics, shape change, biomass, hydrogel, degradable*

Downloaded via Jared Gibson on November 5, 2025 at 21:08:46 (UTC).
See https://pubs.acs.org/sharingguidelines for options on how to legitimately share published articles.

## INTRODUCTION

Engineered living materials (ELMs) integrate living and nonliving components to achieve functional composites with properties that cannot be achieved with either component alone. Frequently, ELMs consist of living microorganisms encapsulated within synthetic materials.[1−3] ELMs can leverage cellular activity to self-repair damage and sense and respond to environmental changes.[4] For example, by embedding load-bearing cement with bacteria, microbially induced mineralization can be used for *in situ* crack repair. Some living infrastructure could also be used for bioremediation.[5−7] Hydrogels that encapsulate engineered bacteria can sense and report the presence of biomolecules or produce drugs on demand.[8] ELMs also enable the manufacturing of materials through biological processes.[9,10] Our previous studies have shown that proliferating microorganisms within a synthetic matrix can cause a material to grow into a programmed form.[11−13] Ultimately, these materials are comprised of over 95% biomass and, therefore, can be designed to readily degrade.[12−14] Using these properties in engineering devices may require ELMs to be interfaced with other functional materials, such as electronic conductors.

Traditional electronics fabrication is comprised of two−dimensional (2D) processes; however, three-dimensional (3D) electronics have applications in a variety of fields from antennas[15,16] to biomedical devices.[17,18] To make 3D electronics, it is necessary to either adjust patterning techniques for 3D substrates or reshape flat substrates into 3D structures after processing. Processes such as stamp printing,[19,20] and additive deposition[21] have demonstrated some ability to pattern directly onto 3D surfaces. However, such methods would necessitate a paradigm shift from the planar patterning approaches currently in use. Thus, many 3D electronic systems utilize planar processing techniques on a flexible substrate which may be wrapped onto a target 3D surface. Such is the case with current electronic systems designed for transient applications. Transient electronics are unique in their ability to partially or fully degrade when no longer needed. However, the functionality of transient electronics, like traditional electronics, is constrained by an inability to manufacture nonplanar electronic devices.[22] While degradable elastomers have been developed to enable stretchable electronics for interfacing with complex-shaped surfaces, a transient substrate which can be patterned in planar form then actuated into an user-defined 3D shape, as seen in alternative nontransient polymer systems, has yet to be developed.[15,23,24] Thus, we propose a system for the

Received: July 31, 2025
Revised: October 14, 2025
Accepted: October 16, 2025

ACS Publications

© XXXX The Authors. Published by American Chemical Society

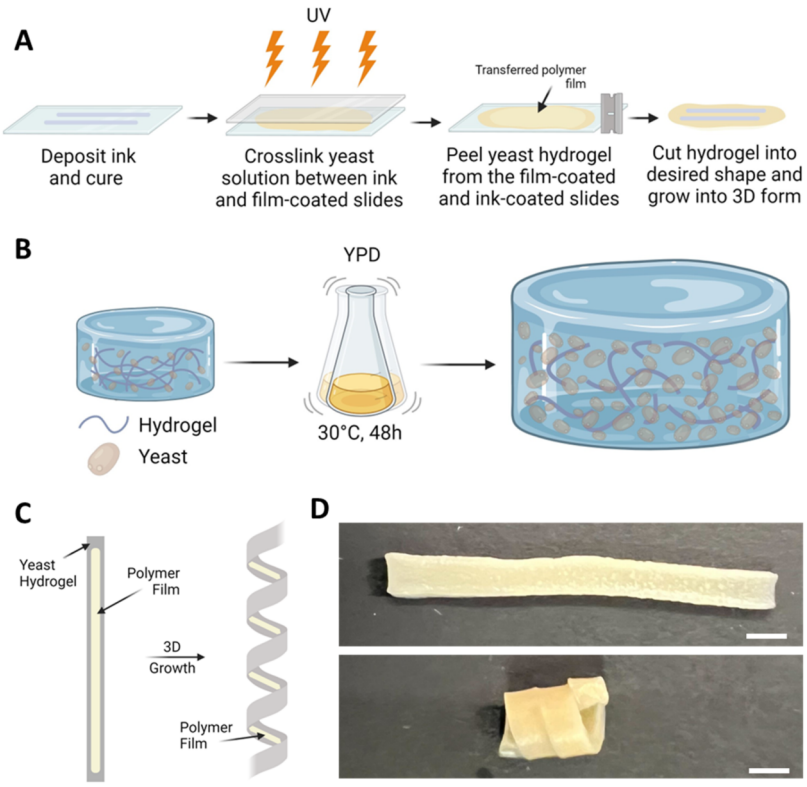


**Figure 1.** (A) Engineered living materials can grow in volume via proliferation of embedded yeast cells. (B) Patterned conductive ink may be transferred onto the hydrogel surface during cross-linking. (C) Strain-guided growth of yeast ELMs by using a stiff polymer coating on one side of the hydrogel. (D) The initially flat film (top) will grow to the desired shape, after 48 h (bottom) (scale bar = 3 mm).

fabrication of transient substrates for 3D electronics using a biodegradable ELM substrate, on which conductive coatings may be transferred onto the substrate in a planar state prior to programmed actuation into 3D form.

Here, we describe the fabrication and characterization of 3D transient electronic substrates from ELMs. Conductive metal inks can be transferred onto the surface of the ELM during cross-linking to fabricate a conductive, largely degradable device (Figure 1A). We compare two different conductive inks on the grown ELM hydrogel and compare the mechanical and electrical properties to inks deposited onto a nonliving substrate. Encapsulated yeast cells proliferate within the hydrogel matrix causing volumetric expansion of the material (Figure 1B). Growth is directed via the use of bilayer mechanics to enable the fabrication of tunable 3D forms (Figure 1C,D). Finally, we demonstrate the degradation of the ELM substrates.

## RESULTS AND DISCUSSION

**Yeast-Induced Growth of ELM Hydrogel.** In this work, our goal is to integrate electronic conductors on ELMs that grow into 3D forms after planar electronics processing. *Saccharomyces cerevisiae*, more commonly known as Baker's yeast, has been shown to proliferate when embedded in a hydrogel matrix and cultured in a nutrient-rich media containing yeast extract, peptone, and dextrose (YPD).[12,13,25] ELM samples were made by dispersing commercially available Baker's yeast and then polymerizing hydroxyethyl acrylate (HEA) and cross-linkers to form a hydrogel matrix as previously described.[13] As the yeast cells proliferate within the hydrogel matrix, an overall increase in volume is observed[12] as the expanding yeast colonies grow in the cross-linked gel matrix and push outward.[13] During this process, microscale fractures are expected to form in the matrix releasing cells into the surrounding media.[26] We note that the chosen yeast strain is commonly used as a food ingredient, and therefore, there is no need for biocontainment. Prior studies using yeast-free hydrogel controls have demonstrated that this process is entirely driven by biological growth, where the magnitude of expansion is a function of initial cell loading and nutrient environment.[12,13] As the biomass content of these ELM substrates increases, changes in mechanical properties such as storage modulus, elastic modulus and glass transition temperature can be observed.[13] These time and composition-dependent properties provide the potential for ELM substrates to be used as a responsive, tunable material system.

In order to make an electronic device that utilizes the physical responsiveness of ELMs, the ELM must be interfaced with conductors and insulators. However, for proliferation to occur, the chosen materials must allow for sufficient nutrient diffusion into the underlying ELM structure. Furthermore, the chosen materials must have low practical cytotoxicity from the electronic materials themselves or from the processing conditions. For this reason, thermally cured inks were avoided to avoid killing the yeast cells. For conductive materials, two types of conductive inks were used. One ink was a particle-free silver ink that can be used to print conductive traces through metal−organic decomposition (MOD). MOD silver ink enables the printing of thin, flexible metal films onto a variety of substrates. MOD inks are being widely explored for electronics processing and fabrication due to their facile processing and potential cost reduction compared to traditional sputtering techniques, such as physical or chemical vapor deposition.[27,28] A second ink utilized was a liquid metal-based


https://doi.org/10.1021/acsapm.5c02855
ACS Appl. Polym. Mater. XXXX, XXX, XXX−XXX

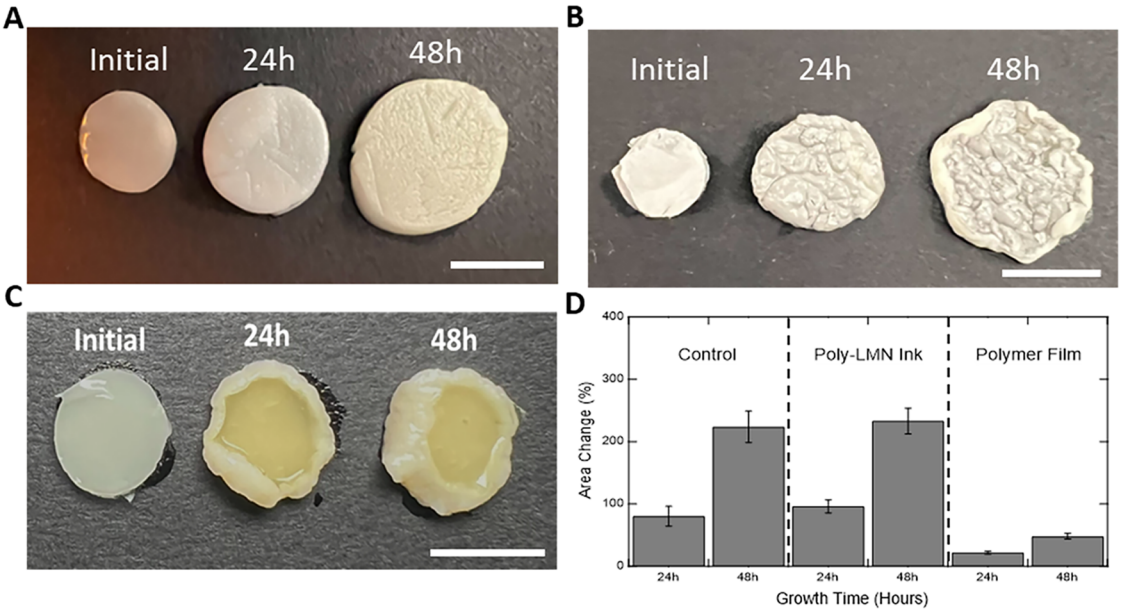


**Figure 2.** (A) Yeast ELM hydrogels grown up to 48 h without coatings (scale bar = 6 mm). (B) Yeast ELMs grown up to 48 h with poly-LMN ink coated on both sides (scale bar = 6 mm). (C) Yeast ELM hydrogels grown for up to 48 h with polymer film on both sides (scale bar = 6 mm). (D) Change in area of ELMs after growth for 24 and 48 h ($n$ = 3, error bars denote standard deviation). The samples are representative images and do not show the same ELM disk over time.

ink comprised of core−shell liquid metal particles. The liquid metal ink was synthesized with an acrylate-functionalized shell to enhance adhesion between particles and with our acrylate-based substrates, which has been previously termed a Polymerized Liquid Metal Network (poly-LMN) ink.[29] The poly-LMN ink was selected for its retention of electrical conductivity under high strains.[29] By using a functionalized polymer shell the poly-LMN particles may be cross-linked to form a cohesive layer upon deposition. This cohesion enables rupturing of the polymer layer under strain, creating an induced conductive network from the liquid metal core. The importance of cross-linking the poly-LMN particles will be further discussed below.

Uncoated ELM discs, ELM discs coated with a stiff polymer film adhered to both sides, or a conductive metal ink coating adhered to both sides were fabricated. For the polymer coating, a glassy, cross-linked film was synthesized using thiol−ene click chemistry.[30] For each of the three coatings, the coating material was first deposited on glass. The ELM was then polymerized in a mold using the coated glass as one of the sides of the mold. The ELM was then dried and removed from the mold. In all cases, the coatings preferentially adhered to the ELM over the glass, transferring the material to the ELM. The adhesion of poly-LMN and EI-1207 silver inks were tested on both the dried yeast-loaded ELM hydrogel and a control non-ELM transient acrylate-based elastomer substrate using ASTM standard D3359. The poly-LMN ink appears to fail a traditional tape test; however, the particulate-based ink does not delaminate as a solid, and instead, a conductive film remains (Figure S1A,B). Thus, the standard adhesion tape test was determined to be inappropriate for comparison in the context of liquid ink. Meanwhile, the silver ink exhibited 4B and 2B adhesion with the ELM and non-ELM substrates, respectively (Figure S1C,D). A rating of 4B indicates good adhesion with less than 5% of the overall surface affected by detachment of the coating.[31] A rating of 2B indicates marginal adhesion to the substrate, with delamination of up to 35%. Cyclical deformation testing on ink-coated substrates proved both inks are flexible but somewhat susceptible to cracking over 5000 deformation cycles as noted by an increase in normalized resistance after deformation (Figures S2 and S3). Detailed results on cyclical deformation testing are available in the Supporting Information.

ELMs partially coated with conductive coatings can still undergo proliferation-induced shape change. Uncoated ELMs exhibited an increased area due to growth of 80 ± 16 and 224 ± 25% following 24 and 48 h of incubation, respectively (Figure 2A). ELMs coated with the silver ink showed that while the ink initially formed a conductive film on the surface of the ELM, the film quickly fragmented upon growth of the substrate (Figure S4). Fragmentation caused a loss of conductivity from a modest 30% increase in area after 12h of growth. Surprisingly, the cross-linked Poly-LMN ink-coated samples, however, exhibited an area growth nearly identical to that of the uncoated samples, with the area increasing by 96.02 ± 10.6% after 24 h and 233.14 ± 20.7% after 48 h (Figure 2B). This coating also does not fragment over the 48 h of incubation in growth media. From these data, it is evident that the poly-LMN ink is, at least initially, permeable to the nutrient media, allowing for cell growth to occur underneath the coating (Figure S5A,B). Poly-LMNs have been demonstrated to initially form a porous network of functionalized particles. As will be discussed below, the growth-induced strain in the material causes the liquid metal droplets to rupture and form a conductive coating, similar to applied strain in elastomer networks initiates this rupture elsewhere.[29] We do not rule out that the ink coatings may cause death of the embedded living material under some conditions. However, we note that the apparent permeability of the poly-LMN coating is encouraging for use in further studies involving conductive living material systems. The polymer coated samples, in contrast, were limited to just 21.9 ± 2.1 and 47.98 ± 4.56% area growth after 24 and 48 h (Figure 2C,D). This may be explained by the limited permeability of the hydrophobic polymer film to the nutrient


https://doi.org/10.1021/acsapm.5c02855
ACS Appl. Polym. Mater. XXXX, XXX, XXX−XXX

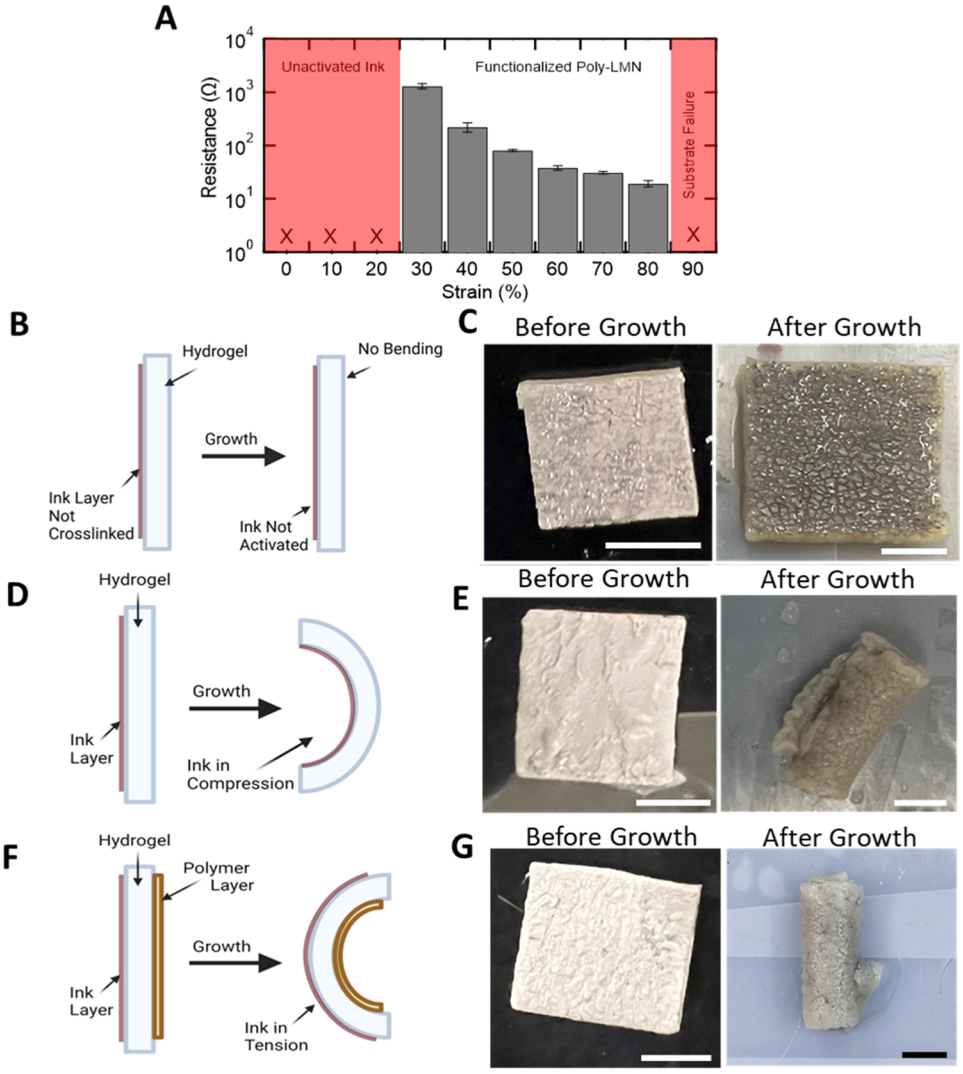


**Figure 3.** (A) Activation of un-cross-linked poly-LMN ink via strain. Red region with X indicates lack of conduction ($n$ = 3, error bars denote standard deviation). (B) Growing the ELM without partially cross-linking the poly-LMN film prior to transfer does not activate the poly-LMN ink. (C) During growth, an un-cross-linked poly-LMN film fragments and does not allow for strain-induced activation (scale bar = 5 mm) (D) Growing hydrogel with a cross-linked Poly-LM layer bends the sample with the ink in compression, limiting activation of the ink. (E) Bending of sample coated with a cross-linked functionalized poly-LMN film (scale bar = 5 mm). (F) Integration of a stiff polymer film redirects bending with the ink layer in tension. (G) A stiff polymer film was cross-linked to the reverse side of the hydrogel, redirecting the bending direction and setting the poly-LMN ink in tension for activation (scale bar = 5 mm).

media necessary for yeast proliferation. In previous studies on yeast metabolism during growth deactivation of yeast cells, or a lack of critical nutrients such as glucose, arrested proliferation and prevented volumetric expansion.[12] This is further evidenced by the uneven growth in the ELM at the edges of the disc, where free diffusion of media enabled rapid growth outward and over the edges of the polymer film (Figure S6). Due to fragmentation of the silver ink during growth, we elected to move forward with the poly-LMN ink for further testing using the ELM substrate, while maintaining the silver ink for use as a control.

The poly-LMN ink is initially nonconductive until activated by deforming of the poly-LMN particles via a process such as stretching, bending, or abrasion. To test the stretch-activation of the poly-LMN ink under applied strain, functionalized particles were partially cross-linked under ultraviolet (UV) light then painted directly onto a predried ELM substrate for mechanical testing. As the initially nonconductive coated substrates were stretched to 30% strain, the poly-LMN particle film was deformed enough to form a conductive network of liquid metal ink, providing a resistance measurement of 1.29 ± 0.15 MΩ. The surface became more conductive as strain increased, with a resistance of 19.4 ± 2.49 Ω at 80% strain (Figure 3A). At strains greater than 80% the dried ELM substrate tended to fracture. These results indicate the adhesion between the ELM substrate and the poly-LMN ink provides the potential for activation during growth where the particles are cross-linked into a cohesive film.

Cross-linking of the poly-LMN particles couples ELM shape with electrical conductivity. The ink was transfer-printed onto the yeast-loaded hydrogels by cross-linking of the ELM substrate. Importantly, we first prepared a coated ELM where the poly-LMN particles are not partially cross-linked prior to transfer printing. The coated ELMs were then placed in growth media. Due to practical limitations, continuous monitoring of electrical properties was unable to be performed


https://doi.org/10.1021/acsapm.5c02855
ACS Appl. Polym. Mater. XXXX, XXX, XXX−XXX

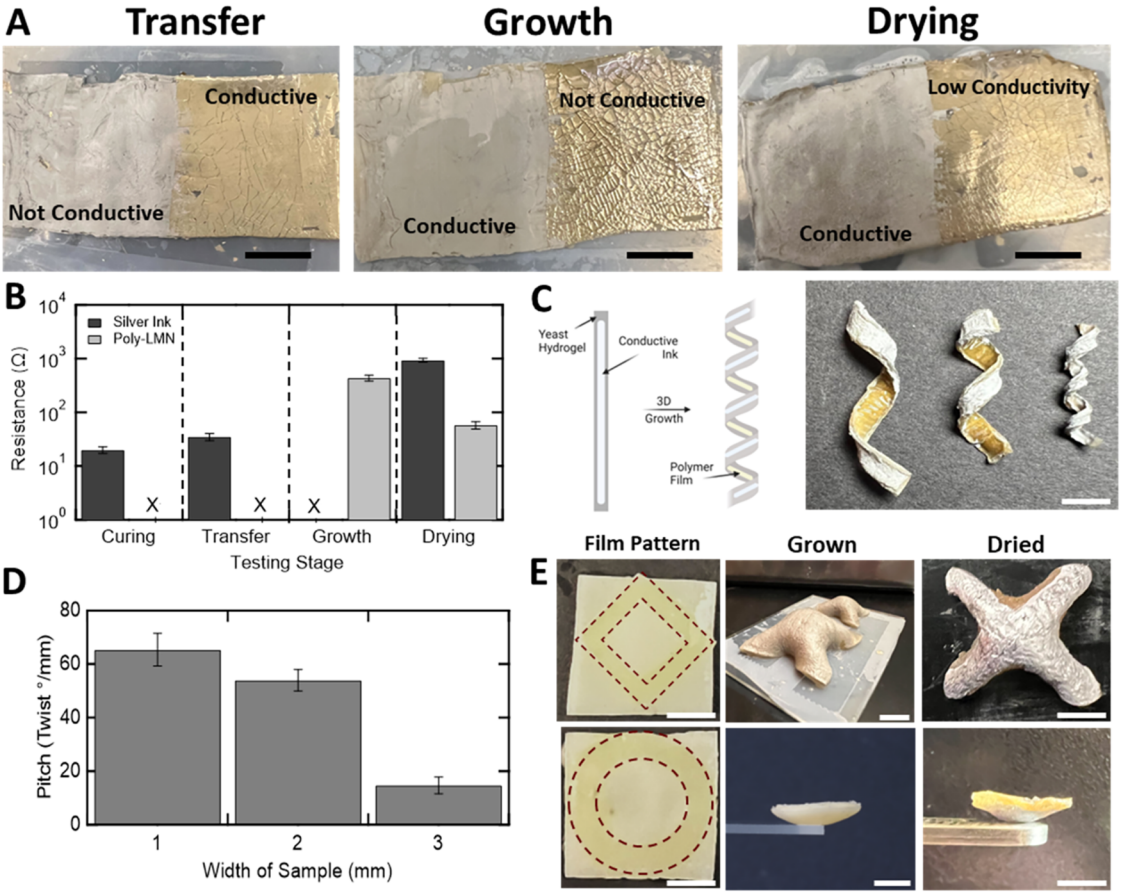


**Figure 4.** (A) ELM sample coated with both poly-LMN (left) and silver inks (right) after ink transfer, after 24 h growth, and after drying. Poly-LMN ink becomes conductive after growth, while the silver ink loses conductivity (scale bar = 10 mm). (B) Resistance measurements for poly-LMN and silver inks after deposition and curing, after transfer to hydrogel, after growth, and after drying ($n$ = 3, error bars note standard deviation). (C) Aspect ratio determines the pitch of bilayer yeast ELMs (scale bar = 3 mm). (D) Pitch of grown bilayer ELMs based on the initial width of a 20 mm long hydrogel ($n$ = 3, error bars denote standard deviation). (E) Various dried forms can be fabricated via directed growth. Dashed lines highlight polymer film pattern for directed growth (scale bar = 3 mm).

during the growth process. Thus, resistance measurements were collected immediately after each stage in the fabrication process; transfer of the coatings onto the ELM surface, after 48 h of growth in YPD media, and after drying. Fragmentation of the poly-LMN coating occurred during growth, resulting in a lack of conductivity (Figure 3B,C). This was hypothesized to be a result of the poly-LMN particles not being cross-linked together prior to transfer, resulting in a noncohesive coating which was unable to transfer the strain generated during growth into the particles during surface expansion. As a result, the poly-LMN particles apparently do not rupture or create a contiguous conductive pathway. By cross-linking the poly-LMN particles together under UV light prior to transfer, a film could be produced to allow for shear-strain activation. In this case, the ink-coated ELM behaves as a bilayer.

**Strain-Guided Shape Change of ELM Substrates.** Bilayers and trilayers comprised of ELMs and coatings undergo programmed growth from 2D to 3D. In bilayers and trilayers with shape-changing layers and passive layers, shape change in one layer causes bending that is controlled by the mechanics of the passive layers.[32,33] Hydrogel bilayer actuators have been studied for use in soft robotics and biomedical devices.[34−36] In ELMs coated with the cross-linked poly-LMN coated on one side, yeast proliferation induces volumetric expansion in the hydrogel layer; and the poly-LMN coating constrains expansion of the adjacent surface. This shape change induces bending with the poly-LMN coating on the inside. As a result, the poly-LMN is in compression (Figure 3D,E). The poly-LMN film requires a minimum amount of strain in tension to create a conductive liquid metal network. To place the poly-LMN coating in tension after growth, we fabricated devices where a polymer film was transferred onto the opposite surface of the ELM as compared to the poly-LMN coating (Figure 3F). This polymer film is stiffer than the poly-LMN coating. During growth of the ELM, this trilayer bends and places the poly-LMN in tension (Figure 3G). This results in electrical conductivity of the poly-LMN film as a result of the growth process that forms the 3D electronic device.

Growth of ELMs can be translated into devices with dynamic electrical conductivity. A 50 mm × 25 mm trilayer ELM substrate was created with polymer film backing and 1/2 coated with silver ink and 1/2 poly-LMN ink on the hydrogel layer via transfer printing (Figure 4A). Two-point resistance measurements were taken using probes spaced at 25 mm across the diagonal of the coated side. After transfer, the silver ink was conductive with a two-point resistance of 35 ± 5.4 Ω. The poly-LMN ink was initially not conductive. Following 48 h growth, the polymer-backed sample was flattened by hand from its curled state that resulted from the growth. The silver ink was found to be fragmented and nonconducting while the


https://doi.org/10.1021/acsapm.5c02855
ACS Appl. Polym. Mater. XXXX, XXX, XXX−XXX

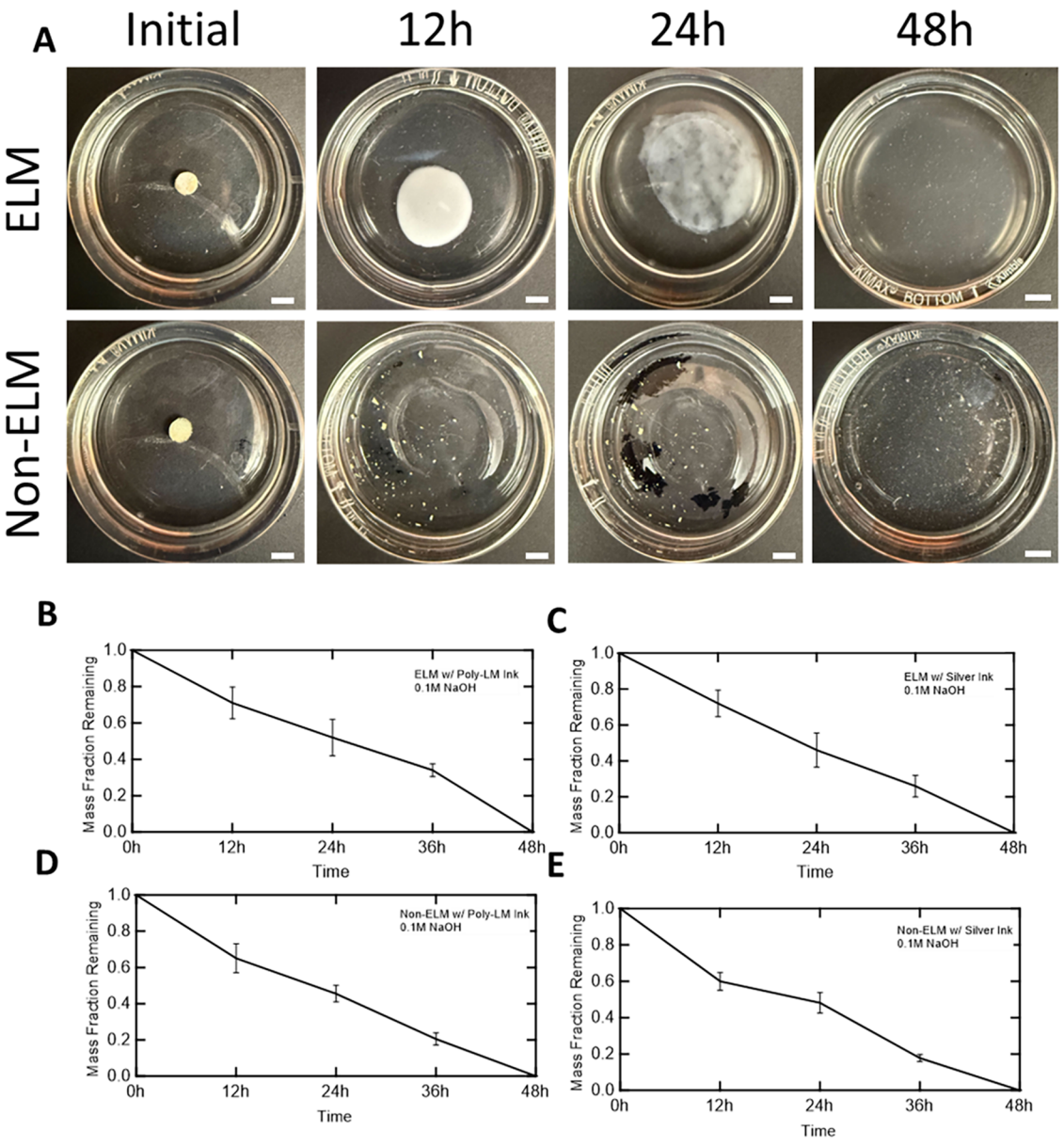


**Figure 5.** (A) Poly-LMN coated ELM (top) and silver coated non-ELM (bottom) hydrogels initially and after 48 h in 0.1 M NaOH (scale bar = 6 mm). (B) Dry mass fraction remaining for silver-coated ELM samples over 48 h in 0.1 M NaOH ($n$ = 3, error bars denote standard deviation). (C) Dry mass fraction remaining for poly-LMN coated ELM samples over 48 h in 0.1 M NaOH ($n$ = 3, error bars denote standard deviation). (D) Dry mass fraction remaining for silver-coated non-ELM samples over 48 h in 0.1 M NaOH ($n$ = 3, error bars denote standard deviation). (E) Dry mass fraction remaining for poly-LMN coated non-ELM samples over 48 h in 0.1 M NaOH ($n$ = 3, error bars denote standard deviation).

poly-LMN ink was conductive with a resistance of 435 ± 53.9 Ω, demonstrating activation via growth of the ELM substrate. After drying overnight at 75 °C, the poly-LMN ink layer demonstrated an 86% decrease in resistance, with the decreased resistance likely due to the shrinkage of the substrate on drying. Shrinkage of the hydrogel due to drying also caused some conductive pathways to be formed in the silver ink layer. The measured resistance after drying was significantly higher than the initial value post-transfer, however (Figure 4B). Fragmentation of the silver ink during growth may enable functionality as a nonreversible on−off switch for environments where yeast growth is activated. Strain activation of the poly-LMN ink by growth, however, enables the potential for activation of the conductive layer during programmed growth into a 3D form.

**3D Characterization and Deformation Testing of Metallized Substrates.** Controlling the aspect ratio of the trilayer ELMs enables fabrication of predictable and tunable 3D forms through growth. In rectangular trilayer systems, a variety of bent forms can be reached based on the aspect ratio of the sample.[37,38] ELMs coated with poly-LMN ink and a stiff polymer film on opposite sides can be cut into rectangular strips of various aspect ratios and grown to form helical structures with tunable pitch (Figure 4C). As the aspect ratio of the sample is decreased by cutting the film into narrow samples of constant length, the pitch of the resulting ELM is increased after growth. ELMs cut with a 3:25 mm aspect ratio exhibited a pitch of 14.7 ± 3.05 °/mm after 48 h of growth and drying. The resulting pitch increases as the aspect ratio is


https://doi.org/10.1021/acsapm.5c02855
ACS Appl. Polym. Mater. XXXX, XXX, XXX−XXX

reduced, with 2:25 mm and 1:25 mm films exhibiting pitches of 54 ± 4 and 65 ± 6 °/mm, respectively (Figure 4D).

Using strain-guided bilayer growth, various complex 3D shapes can be fabricated by altering the spatial pattern of the stiff polymer coating on the ELM. A convex "X" shape was formed by cutting the polymer backing layer into a hollow diamond design before transfer. By transferring the poly-LMN ink onto the opposite side of the substrate before growth, the form can be made conductive on the surface, with a functional 3D conductor fabricated upon drying. Likewise, a hemispherical form can be grown into 3D by transferring an "O" pattern of polymer film onto the ELM. The substrate can be grown into a hemispherical form. In both of these shapes, expansion in area in the regions of the ELM without the stiff polymer backing leads to the 3D form. The ELMs retain this shape upon drying (Figure 4E). Using this simple fabrication approach, combined with growth-induced activation of the poly-LMN ink, we envision a substantial library of conductive 3D forms to be achievable. While we anticipate a variety of potential uses for this platform to produce 3D electronics, we note that further investigation is needed to characterize yeast-based ELMs as a useful dielectric material. The hydrophilic nature of the ELM, which related to the use of a biomass-based platform, may limit the potential for use in some environments.

**Degradation of ELM Substrates.** ELMs that are comprised largely of biomass are particularly suitable for decomposition at the end of their functional lifespan. Our previous work has demonstrated that these yeast-based ELMs degrade, and the degradation time is determined by the chosen cross-linker for the system.[13] To allow for hydrolytic degradation of our chosen polymer matrices, aliphatic ester-containing cross-linker polyethylene glycol diacrylate (PEGDA) was utilized as the cross-linker for synthesizing degradable ELM and non-ELM substrates. It has been previously demonstrated that the choice of cross-linker has no substantial effect on cell viability and growth of the living material.[13] Testing in accelerated degradation conditions using 0.1 M sodium hydroxide (NaOH) demonstrated the total loss of integrity for both the ELM substrate and non-ELM substrate within 48 h (Figure 5A). While the silver ink gradually fractured over the degradation period, trace amounts were visible after complete substrate degradation. During degradation testing of the poly-LMN coated substrates, the ink tended to delaminate from the degrading substrate and coalesce in the solution, remaining suspended even after full dissolution of the substrate. Limited degradation of the poly-LMN ink may be attributed to the use of 11-phosphonoundecyl acrylate as the polymer coating, where this hydrophobic polymer is more resistant to hydrolysis than the ELM substrate.[29,39] In the context of waste management, the potential environmental impact of the inks should also be addressed, as the inks are not expected to be degraded during the substrate degradation. Silver is toxic in some scenarios.[40] On the contrary, EGaIn liquid metal is generally known to exhibit low toxicity, with use in biomedical applications.[41,42] Any future application would require further evaluation of the degradation products and inks.

The conductive ink coatings were demonstrated to have no discernible impact on the degradation of the polymer substrates. A similar degradation profile is observed for both the silver-coated and poly-LMN coated ELM substrates over the course of 48 h, where no solid mass remained in the accelerated hydrolytic solution (Figure 5B,C). Here, we note that the use of a far lower concentration of PEGDA in our ELM substrate than in previous studies allows for more rapid dissolution of the substrate.[13,43] Degradation of the non-ELM substrate remained consistent across both conductive coatings (Figure 5D,E). While testing was performed in accelerated conditions, NaOH is not expected to be required for hydrolytic degradation of the transient substrates. Degradation in more neutral environments provides a potential avenue for these materials to be used as waste-reducing electronic substrates.[44]

## CONCLUSION

Conductive metal inks can be patterned onto degradable substrates for the potential fabrication of transient electronics. The use of a yeast-based ELM allows for the bilayer actuation of ink-coated substrates into conductive 3D forms, enabling the fabrication of complex-curved shapes while retaining compatibility with current transfer printing methods. Compatibility of the hydrolytically degradable ELM with conductive components presents a promising avenue for the development of transient 3D electronics. By expanding the functionality of transient electronics, this research seeks to contribute a potential future strategy for the reduction of global e-waste in our oceans and landfills.

## MATERIALS AND METHODS

**Synthesis of ELM and Non-ELM Substrates.** Yeast-based hydrogel samples were synthesized via a one-pot mixture of 17.5 wt % hydroxyethyl acrylate (HEA), 10 wt % of a 2 wt % *N*,*N*-methylenebis(acrylamide) (MBAm) stock solution, 45.5 wt % DI water, 23.5 wt % commercially available Baker's yeast, and 3.5 wt % Lithium phenyl-2,4,6-trimethylbenzoylphosphinate (LAP) as the cross-linker. The solution was then pipetted between two RainX coated slides with a 1 mm glass spacer between them. The glass cell was then placed in a UV chamber and cross-linked under 365 nm light with 10 mW/cm$^2$ intensity for 2 min, flipping every 30 s. For the yeast samples with ink on both sides, photo-cross-linking was hindered by the ink layer, necessitating the use of a thermal cross-linking composition. In this case, the LAP was replaced with 3.5 wt % of a 10 wt % ammonium persulfate (APS) solution and 5 vol % of tetramethyl ethylenediamine (TEMED) and allowed to cure for 20 min, flipping every 2 min to avoid sedimentation of yeast. In both cases, samples were washed in DI water before being placed in YPD media and put in an incubating shaker at 30 °C. Media was changed every 24 h.

For the non-ELM substrates, a solution of 95 wt % HEA, 5 wt % of a 9.1 wt % polyethylene glycol diacrylate (PEGDA, 500 Mn, stock solution), and 0.2 wt % Irgacure 369 was mixed and pipetted between two RainX coated slides with a 1 mm spacer. The glass cells were cross-linked for 20 min in a 365 nm UV chamber with 10 mW/cm$^2$ intensity, flipping every 5 min.

**Transfer of Conductive Inks.** For the silver ink, EI-1207 ink was selected due to its low adhesion to glass, enabling conductive films to be deposited onto glass substrates and transfer-printed onto the target transient substrate. EI-1207 was deposited via spray coating onto a glass slide by Electroninks and sent to TAMU. The desired trace pattern, if any, was achieved by scraping the silver ink using a razor. Silver ink was transferred to ELM samples by replacing one glass slide in the cell with a silver-coated slide and cross-linking via UV, making sure to first cross-link through the noncoated slide. The cross-linked substrate was submerged in DI water and the noncoated slide removed. A razor was then used to guide the delamination of the ink-coated slide from the glass. For the non-ELM samples, EI-1207 was directly spray coated and cured onto the substrates by Electroninks.

Poly-LMN ink was provided by AFRL dispersed in ethanol. Before use unless otherwise defined, the poly-LMN ink particles were cross-linked by transferring the solution to a glass container and exposing to 15 mW/cm$^2$ 365 nm UV light for 5 min. Glass slides were heated to


https://doi.org/10.1021/acsapm.5c02855
ACS Appl. Polym. Mater. XXXX, XXX, XXX−XXX

80 °C and cross-linked poly-LMN ink solution was brushed onto the surface of the slide using a paintbrush. Poly-LMN ink was cured for 20 min to allow the ethanol to evaporate, leaving the poly-LMN film behind. The ink was then transferred to the ELM samples using the previously described process. For non-cross-linked poly-LMN ink, the process was identical except the UV light exposure was omitted.

**Adhesion Testing of Inks on Degradable Substrates.** The adhesion of poly-LMN and EI-1207 silver inks were tested on both the yeast-loaded ELM hydrogel and a control non-ELM transient acrylate-based elastomer substrate using ASTM standard D3359. The poly-LMN ink received a 0B rating on both the ELM and non-ELM substrates, indicating poor adhesion to the surface (Figure S1A,B). However, due to shear-activation of the poly-LMN ink, delamination of the surface layer caused the ink to become conductive, where the base layer of ink remaining on the surface of the substrate exhibited resistances as low as 0.3 Ω. Thus, while the ink appears to fail a traditional tape test, the activation of a conductive base layer on the substrate surface indicates viability for use in both the 3D ELM system and for a nondeforming transient substrate. Meanwhile, the silver ink exhibited 4B and 2B adhesion with the ELM and non-ELM substrates, respectively (Figure S1C,D). In accordance to ASTM D3359, a rating of 4B indicates good adhesion with less than 5% of the overall surface affected by detachment of the coating.[30] A rating of 2B indicates marginal adhesion to the substrate, with delamination of up to 35%. Despite previously reported fragmentation during growth, these results indicate the silver ink to be a strong candidate for use with the ELM substrate as a transient conductor if not grown.

**Fabrication of Strain-Guided ELMs and Growth.** To fabricate the strain-guided samples for 3D growth, the ELM solution was cross-linked between a glass slide coated with poly-LMN ink and a glass slide spin-coated at 1500 rpm with a thin film containing a 1:1 molar ratio of pentaerythritol tetrakis(3-mercaptopropionate) (PETMP) to ethylenedioxy diethanethiol (EDDT), where the film adhered to the hydrogel and could be delaminated from the glass slides. After cross-linking, the samples were washed with DI water and cut to the desired size with a razor. The cut samples were then placed in YPD media and grown for 48 h, changing the media every 24 h. For more helical samples, the entire ELM substrate was backed with polymer and cut into strips of the desired width for growth. For the more complex shapes, the polymer coating was cut into the desired shape before cross-linking and transfer, and the ELM substrate was cut to the size of the polymer backing. Samples were dried for 2h in a 70 °C oven, then removed and air-dried for 24−48 h. Samples were dried on Teflon-coated slides to prevent sticking.

**Deformation Testing.** Cyclical deformation testing was performed using a dynamic mechanical analyzer (DMA). Samples were cut into 25 mm × 2 mm strips and loaded at room temperature. For testing strain activation of the ink, samples were strained at a rate of 100% strain in 60s, stopping at every 10% strain for a resistance measurement. For cyclical deformation testing of the ink-coated substrates, samples were compressed by 20% of their original length, making sure to put the ink on the outside of the curve, and repeated at a frequency of 1 Hz for 1000 and 5000 cycles. Separate samples were used for 1000 and 5000 cycle testing. Images of the ink surface were taken using a polarizing optical microscope (POM) in reflectance mode. Resistance measurements were determined by taking the average of three samples taken from individual batches.

**Accelerated Degradation of Substrates.** Accelerated hydrolytic conditions were formed using 0.1 M sodium hydroxide (NaOH). To fabricate a degradable substrate, MBAm was replaced with an equivalent weight percent of PEGDA in the ELM substrates. ELM and non-ELM samples were prepared as described above then punched into 4 mm discs. ELM samples were dried in a 70 °C oven overnight before punching into disks. The dry mass of each disk was weighed initially, then the discs were placed into individual vials filled with 20 mL of 0.1 M NaOH. Vials were placed on a shake plate at room temperature and agitated at 20 rpm. Time points were taken at 12, 24, 36, 48, and 72 h, where samples were removed from solution and dried in an oven at 70 °C overnight to remove any liquid content. The remaining dry mass fraction of the discs was used for comparison. Discs which demonstrated complete loss of integrity when attempting to handle were designated as fully degraded. After drying, discs were not reused for further time points. Three discs from independent batches were utilized for each time point.

## ■ ASSOCIATED CONTENT

### Supporting Information

The Supporting Information is available free of charge at https://pubs.acs.org/doi/10.1021/acsapm.5c02855.

Additional characterization of ink-substrate adhesion, growth of ink-coated ELMs, and cyclical deformation testing (PDF)

## ■ AUTHOR INFORMATION


### Corresponding Author

**Taylor H. Ware** − *Department of Biomedical Engineering, Texas A&M University, College Station, Texas 77840, United States; Department of Materials Science and Engineering, Texas A&M University, College Station, Texas 77840, United States;* orcid.org/0000-0001-7996-7393; Email: taylor.ware@tamu.edu

### Authors

**Jared A. Gibson** − *Department of Biomedical Engineering, Texas A&M University, College Station, Texas 77840, United States;* orcid.org/0009-0000-5005-8532

**Sasha M. George** − *Department of Materials Science and Engineering, Texas A&M University, College Station, Texas 77840, United States;* orcid.org/0009-0007-8640-3343

**Cedric P. Ambulo** − *Electroninks Incorporated, Austin, Texas 78744, United States*

**Manivannan Sivaperuman Kalairaj** − *Department of Biomedical Engineering, Texas A&M University, College Station, Texas 77840, United States;* orcid.org/0000-0002-3218-7135

**Yoo Jin Lee** − *Department of Biomedical Engineering, Texas A&M University, College Station, Texas 77840, United States*

**Melbs LeMieux** − *Electroninks Incorporated, Austin, Texas 78744, United States*

**Christopher E. Tabor** − *Air Force Research Laboratory, Dayton, Ohio 45433, United States*

Complete contact information is available at: https://pubs.acs.org/10.1021/acsapm.5c02855


### Author Contributions

The manuscript was written through contributions of all authors. All authors have given approval to the final version of the *manuscript*.

### Notes

The authors declare no competing financial interest.

## ■ ACKNOWLEDGMENTS

This material is based upon work supported by the Air Force Research Laboratory/AFWERX under Contract No. FA864922P0824. The authors would also like to acknowledge the use of the Materials Characterization Facility (RRID: SCR_022202) at Texas A&M University.

## ■ REFERENCES

(1) Chen, A. Y.; Zhong, C.; Lu, T. K. Engineering Living Functional Materials. *ACS Synth. Biol.* **2015**, *4*, 8−11.

(2) Gilbert, C.; Ellis, T. Biological Engineered Living Materials: Growing Functional Materials with Genetically Programmable Properties. *ACS Synth. Biol.* **2019**, *8*, 1−15.
(3) Rodrigo-Navarro, A.; Sankaran, S.; Dalby, M. J.; del Campo, A.; Salmeron-Sanchez, M. Engineered living biomaterials. *Nat. Rev. Mater.* **2021**, *6*, 1175−1190.
(4) Caro-Astorga, J.; Walker, K. T.; Herrera, N.; Lee, K.-Y.; Ellis, T. Bacterial cellulose spheroids as building blocks for 3D and patterned living materials and for regeneration. *Nat. Commun.* **2021**, *12*, No. 5027.
(5) Xu, J.; Yao, W. Multiscale mechanical quantification of self-healing concrete incorporating non-ureolytic bacteria-based healing agent. *Cem. Concr. Res.* **2014**, *64*, 1−10.
(6) Datta, D.; Weiss, E. L.; Wangpraseurt, D.; Hild, E.; Chen, S.; Golden, J. W.; Golden, S. S.; Pokorski, J. K. Phenotypically complex living materials containing engineered cyanobacteria. *Nat. Commun.* **2023**, *14*, No. 4742.
(7) Chen, G.; Liang, X.; Zhang, P.; Shaoting, L.; Chengcheng, C.; Ziyi, Y.; Liu, J. Bioinspired 3D Printing of Functional Materials by Harnessing Enzyme-Induced Biomineralization. *Adv. Funct. Mater.* **2022**, *32*, No. 2113262.
(8) Han, C.; Zhang, X.; Pang, G.; Zhang, Y.; Pan, H.; Li, L.; Cui, M.; Liu, B.; Kang, R.; Xue, X.; Sun, T.; Liu, J.; Chang, J.; Zhao, P.; Zhao, P.; Wang, H. Hydrogel microcapsules containing engineered bacteria for sustained production and release of protein drugs. *Biomaterials* **2022**, *287*, No. 121619.
(9) Johnston, T. G.; Yuan, S.-F.; Wagner, J.; Yi, Y.; Saha, A.; Smith, P.; Nelson, A.; Alper, H. Compartmentalized microbes and co-cultures in hydrogels for on-demand bioproduction and preservation. *Nat. Commun.* **2020**, *11*, No. 563.
(10) Kang, S.-Y.; Pokhrel, A.; Bratsch, S.; Benson, J. J.; Seo, S.-O.; Quin, M.; Aksan, A.; Schmidt-Dannert, C. Engineering Bacillus subtilis for the formation of a durable living biocomposite material. *Nat. Commun.* **2021**, *12*, No. 7133.
(11) Gilbert, C.; Tang, T.-C.; Ott, O.; Dorr, B. A.; Shaw, W. M.; Sun, G. L.; Lu, T. K.; Ellis, T. Living materials with programmable functionalities grown from engineered microbial co-cultures. *Nat. Mater.* **2021**, *20*, 691−700.
(12) Rivera-Tarazona, L. K.; Bhat, V. D.; Kim, H.; Campbell, Z. T.; Ware, T. H. Shape-morphing living composites. *Sci. Adv.* **2020**, *6*, No. eaax8582.
(13) Wang, S.; Rivera-Tarazona, L. K.; Abdelrahman, M. K.; Ware, T. H. Digitally Programmable Manufacturing of Living Materials Grown from Biowaste. *ACS Appl. Mater. Interfaces* **2022**, *14*, 20062−20072.
(14) Ates, H. C.; Nguyen, P. Q.; Gonzalez-Macia, L.; Morales-Narváez, E.; Güder, F.; Collins, J. J.; Dincer, C. End-to-end design of wearable sensors. *Nat. Rev. Mater.* **2022**, *7*, 887−907.
(15) Kim, H.; Gibson, J.; Maeng, J.; Saed, M. O.; Pimentel, K.; Rihani, R. T.; Pancrazio, J. J.; Georgakopoulos, S. V.; Ware, T. H. Responsive, 3D Electronics Enabled by Liquid Crystal Elastomer Substrates. *ACS Appl. Mater. and Interfaces* **2019**, *11*, 19506−19513.
(16) Zhu, J.; Hu, Z.; Zhang, S.; Zhang, X.; Zhou, H.; Xing, C.; Guo, H.; Qiu, D.; Yang, H.; Song, C.; Cheng, H. Stretchable 3D Wideband Dipole Antennas from Mechanical Assembly for On-Body Communication. *ACS Appl. Mater. Interfaces* **2022**, *14*, 12855−12862.
(17) Kim, J.; Kim, M.; Lee, M.-S.; Kim, K.; Ji, S.; Sangyoon, J.; Kim, Y.-T.; Park, J.; Na, K.; Bae, K.-H.; Kim, H. K.; Bien, B.; Lee, C. Y.; Park, J.-U. Wearable smart sensor systems integrated on soft contact lenses for wireless ocular diagnostics. *Nat. Commun.* **2017**, *8*, No. 14997.
(18) Fan, J. A.; Yeo, W.-H.; Su, Y.; Hattori, Y.; Lee, W.; Jung, S.-Y.; Zhang, Y.; Liu, Z.; Cheng, H.; Falgout, L.; Bajema, M.; Coleman, T.; Gregoire, D.; Larsen, R. J.; Huang, Y.; Rogers, J. A. Fractal design concepts for stretchable electronics. *Nat. Commun.* **2014**, *5*, No. 3266.
(19) Parker, M. Petal-like stamps make curvy devices. *Nat. Electron.* **2023**, *6*, 551.
(20) Sim, K.; Chen, S.; Li, Z.; Rao, Z.; Liu, J.; Lu, Y.; Jang, S.; Ershad, F.; Chen, J.; Xiao, J.; Yu, C. Three-dimensional curvy electronics created using conformal additive stamp printing. *Nat. Electron.* **2019**, *2*, 471−479.
(21) Hong, F.; Lampret, B.; Myant, C.; Hodges, S.; Boyle, D. 5-axis multi-material 3D printing of curved electrical traces. *Addit. Manuf.* **2023**, *70*, No. 103546.
(22) Chien, A. A.; Abowd, G. D.; Oh, H.; Hester, J. Transient Internet of Things: Redesigning the Lifetime of Electronics for a More Sustainable Networked Environment. *Proc. 2nd Work. Sustain. Comput. Syst.* **2023**, *18*, 1−8.
(23) Han, W. B.; Ko, G.-J.; Lee, K.-G.; Kim, D.; Lee, J. H.; Yang, S. M.; Kim, D.-J.; Shin, J.-W.; Jang, T.-M.; Han, S.; Zhou, H.; Kang, H.; Lim, J. H.; Rajaram, K.; Cheng, H.; Park, Y.-D.; Kim, S. H.; Hwang, S.-W. Ultra-stretchable and biodegradable elastomers for soft, transient electronics. *Nat. Commun.* **2023**, *14*, No. 2263.
(24) Huang, Q.; Tang, B.; Romero, J. C.; Yang, Y.; Elsayed, S. K.; Pahapale, G.; Lee, T.-J.; Pantoja, I. E. M.; Han, F.; Berlinicke, C.; Xiang, T.; Solazzo, M.; Hartung, T.; Qin, Z.; Caffo, B. S.; Smirnova, L.; Gracias, D. Shell Microelectrode Arrays (MEAs) for brain organoids. *Sci. Adv.* **2022**, *8*, No. eabq5031.
(25) Saha, A.; Johnston, T. G.; Shafranek, R. T.; Goodman, C. J.; Zalatan, J. G.; Storti, D. W.; Ganter, M. A.; Nelson, A. Additive Manufacturing of Catalytically Active Living Materials. *ACS Appl. Mater. Interfaces* **2018**, *10*, 13373−13380.
(26) Kalairaj, M. S.; George, I.; George, S. M.; Farfán, S. E.; Lee, Y. J.; Rivera-Tarazona, L. K.; Wang, S.; Abdelrahman, M. K.; Tasmim, S.; Dana, A.; Zimmern, P. E.; Subashchandrabose, S.; Ware, T. H. Controlled Release of Microorganisms from Engineered Living Materials. *ACS Appl. Mater. Interfaces.* **2025**, *17* (28), 40326−40339.
(27) Farr, N. T. H.; Davies, M.; Nohl, J.; Abrams, K. J.; Schäfer; Yufang, L.; Gerling, T.; Stehling, N.; Mehta, D.; Zhang, J.; Mihaylova, L.; Wilmott, J. R.; Black, K.; Rodenburg, C. Revealing The Morphology of Ink and Aerosol Jet Printed Palladium-Silver Alloys Fabricated from Metal Organic Decomposition Inks. *Adv. Sci.* **2024**, *11*, No. 2306561.
(28) Kell, A. J.; Wagner, K.; Liu, X.; Lessard, B. H.; Paquet, C. Advanced Applications of Metal−Organic Decomposition Inks in Printed Electronics. *ACS Appl. Electron. Mater.* **2024**, *6*, 1−23.
(29) Farrell, Z. J.; Thrasher, C. J.; Flynn, A. E.; Tabor, C. E. Silanized Liquid-Metal Nanoparticles for Responsive Electronics. *Appl. Nano. Mater.* **2020**, *3*, 6297−6303.
(30) Le May, I.; Lappi, V. G.; White, W. E. Materials for biomedical applications. *Polym. Eng. Sci.* **1975**, *15*, 789−794.
(31) *Standard Test Methods for Rating Adhesion by Tape Test*, ASTM D3359−232023.
(32) Tang, L.; Wu, X.; Xu, Y.; Li, Y.; Wu, S.; Gong, L.; Tang, J. Bilayer Hydrogel Actuators with High Mechanical Properties and Programmable Actuation via the Synergy of Double-Network and Synchronized Ultraviolet Polymerization Strategies. *Polymers* **2024**, *16*, No. 840.
(33) Basak, S.; Bandyopadhyay, A. Next-gen biomimetic actuators: bilayer hydrogel evolution in the 21st century and its advancements from a post-2020 perspective. *RSC Appl. Polym.* **2024**, *2*, 583−605.
(34) Liman, G.; Mutluturk, E.; Demirel, G. Light- and Solvent-Responsive Bilayer Hydrogel Actuators with Reversible Bending Behaviors. *ACS Mater. Au* **2024**, *4*, 385−392.
(35) Liu, W.; Geng, L.; Wu, J.; Huang, A.; Peng, X. Highly strong and sensitive bilayer hydrogel actuators enhanced by cross-oriented nanocellulose networks. *Compos. Sci. Technol.* **2022**, *225*, No. 109494.
(36) Duan, J.; Liang, X.; Zhu, K.; Guo, J.; Zhang, L. Bilayer hydrogel actuators with tight interfacial adhesion fully constructed from natural polysaccharides. *Soft Matter* **2017**, *13*, 345−354.
(37) Alben, S.; Balakrisnan, B.; Smela, E. Edge Effects Determine the Direction of Bilayer Bending. *Nano Lett.* **2011**, *11*, 2280−2285.
(38) Chun, I. S.; Challa, A.; Derickson, B.; Hsia, K. J.; Li, X. Geometry Effect on the Strain-Induced Self-Rolling of Semiconductor Membranes. *Nano Lett.* **2010**, *10*, 3927−3932.
(39) Harsági, N.; Keglevich, G. The Hydrolysis of Phosphinates and Phosphonates: A Review. *Molecules* **2021**, *26*, No. 2840.


https://doi.org/10.1021/acsapm.5c02855
*ACS Appl. Polym. Mater.* XXXX, XXX, XXX−XXX

(40) Padhye, L. P.; Jasemizad, T.; Bolan, S.; Tsyusko, O. V.; Unrine, J. M.; Biswal, B. K.; Balasubramanian, R.; Zhang, Y.; Zhang, T.; Zhao, J.; Li, Y.; Rinklebe, J.; Wang, H.; Siddique, K. H. M.; Bolan, N. Silver contamination and risk management in terrestrial and aquatic ecosystems. *Sci. Total Environ.* **2023**, *871*, No. 161926.
(41) Deng, Y.; Bu, F.; Wang, Y.; Chee, P. S.; Liu, X.; Guan, C. Stretchable liquid metal based biomedical devices. *npj Flexible Electron.* **2024**, *8*, No. 12.
(42) Yan, J.; Lu, Y.; Chen, G.; Yang, M.; Gu, Z. Advances in liquid metals for biomedical applications. *Chem. Soc. Rev.* **2018**, *47*, 2518−2533.
(43) Krongauz, V. V. Crosslink density dependence of polymer degradation kinetics: Photocrosslinked acrylates. *Thermochim. Acta* **2010**, *503-504*, 70−84.
(44) Kim, H.; Townsend, T. G. Wet landfill decomposition rate determination using methane yield results for excavated waste samples. *Waste Manage.* **2012**, *32*, 1427−1433.



https://doi.org/10.1021/acsapm.5c02855
ACS Appl. Polym. Mater. XXXX, XXX, XXX−XXX